

Supporting Information

Mechanism of H₂ Evolution from a Phototriggered Hydridocobaloxime

Jillian L. Dempsey, Jay R. Winkler, Harry B. Gray

1. Synthetic Details	S2
2. Photochemical Measurements	S3
3. Calculations of Ground State and Excited State p <i>K</i> _a Values	S8
4. Hydrogen Yields from Bulk Photolysis	S10
5. Calculation of barriers.....	S11

1. Synthetic Details

General methods

Syntheses of air and moisture sensitive compounds were carried out in a nitrogen atmosphere glovebox. Solvents for these syntheses were dried by a standard method¹ or over activated sieves followed by passage over activated alumina. CD₃CN was obtained from Cambridge Isotope Laboratories, Inc. All materials, unless noted, were used as received. Tetrabutylammonium hexafluorophosphate and 6-bromo-2-naphthol were purchased from Aldrich and recrystallized from ethanol. Co(dm_gBF₂)(CH₃CN)₂ was prepared according to the method of Bakac and Espenson.² MeCo(dm_gBF₂)₂(CH₃CN) was prepared by the method of Ram et al.³ NMR spectra were recorded using a Varian Mercury 300 spectrometer. ¹H NMR chemical shifts were referenced to residual solvents as determined relative to Me₄Si (δ=0 ppm).

[Na][Co(dm_gBF₂)₂(CH₃CN)]

[Na][Co(dm_gBF₂)₂(CH₃CN)] was prepared in an analogous method to the literature preparation for [Na][Co(dpgBF₂)₂(CH₃CN)].⁴ 0.251 g (0.559 mmol, 1 eq.) of Co(dm_gBF₂)(CH₃CN)₂ was suspended in 4 mL of THF and transferred to a 20 mL scintillation vial containing 2.673 g (0.579 mmol, 1.04 eq.) of sodium mercury amalgam (0.5% Na). The reaction was stirred for 3 hours to yield a deep blue-black solution. Solution was removed from the mercury and remaining blue solid was dissolved in CH₃CN and removed. THF and CH₃CN solutions were mixed and the solvent was reduced to <1 mL. 15 mL of Et₂O was added to precipitate a blue solid, which was collected via filtration on medium frit. Product was dried under vacuum. Yield =71%. ¹H NMR (CD₃CN, 300 MHz): δ 2.09 (s, 12H), 1.96 (s, 3H).

Sodium 6-Bromo-2-Naphtholate

In an inert atmosphere, a 20 mL scintillation vial was charged with 21 mg (0.883 mmol) sodium hydride and a stirbar. A solution of 197 mg (0.883 mmol) of 6-bromo-2-naphthol in 4 mL dry, degassed acetonitrile, was transferred to the reaction vessel. A white suspension was immediately formed and vigorous bubbling was observed. Reaction was allowed to stir for 1 hour, until solution became clear pale yellow. Solution was filtered and solvent was removed. Yield = 90%. ¹H NMR (CD₃CN, 300 MHz): δ 7.67 (d, J = 1.2 Hz, 1H), 7.39 (d, J = 8.7 Hz, 1 H), 7.18 (m, 2H), 6.92 (dd, J₁ = 8.9 Hz, J₂ = 2.6 Hz, 1H), 6.66 (d, J = 2.4 Hz, 1H)

2. Photochemical Measurements

Photochemical Methods

UV-visible absorption measurements were carried out using a Hewlett Packard 8452 or Cary 50 UV-Vis spectrophotometer in 1 cm pathlength quartz cuvettes.

Samples for transient absorption and room temperature luminescence measurements were prepared in dry, degassed CH₃CN and placed into the cell of a high-vacuum 1-cm pathlength fused quartz cuvette (Starna Cells) connected to a 10 mL bulb and isolated from atmosphere and the bulb by a high-vacuum Teflon valve (Kontes). Samples for low temperature luminescence measurements were prepared in dry, degassed butyronitrile and placed in 1 cm diameter glass tubes sealed with a high-vacuum Teflon valve.

Steady-state and time-resolved spectroscopic measurements were carried out at the Beckman Institute Laser Resource Center (California Institute of Technology). Emission spectra were recorded on a Jobin Yvon Spec Fluorolog-3-11. Sample excitation was achieved via a xenon arc lamp with wavelength selection provided by a monochromator. Right angle emission was sorted using a monochromator and detected with a Hamamatsu R928P photomultiplier tube with photon counting. Appropriate long pass filters were utilized to minimize scattered excitation wavelength. Low temperature measurements were made in a liquid nitrogen filled glass finger dewar aligned in the fluorometer sample cavity.

For time-resolved measurements, 266 nm laser excitation was provided by 8 ns pulses from the fourth harmonic of a 10 Hz Q-switched Nd:YAG laser (Spectra-Physics Quanta-Ray PRO-Series). Probe light for transient absorption kinetics measurements was provided by a 75-W arc lamp (PTI Model A 1010) that could be operated in continuous wave or pulsed modes. Timing between the laser and the probe light was controlled by a digital delay generator. After passing through the sample collinearly with the laser beam, scattered excitation light was rejected by suitable long pass and short pass filters, and probe wavelengths were selected for detection by a double monochromator (Instruments SA DH-10) with 1 mm slits. Transmitted light was detected with a photomultiplier tube (PMT, Hamamatsu R928). The PMT current was amplified and recorded with a GageScope transient digitizer. The data were converted to units of ΔOD ($\Delta OD = -\log_{10}(I/I_0)$, where I is the time-resolved probe-light intensity with laser excitation, and I_0 is the intensity without excitation). Samples measured on the microsecond timescale or faster were stirred continuously and measured using a laser repetition rate of 10 Hz, while

samples measured on a millisecond timescale were excited with a single shutter-released laser pulse, stirred for 1 s after collecting data, then allowed to sit until the solution settled (2 s) before the next laser pulse. Data were averaged over approximately 50 shots. All instruments and electronics in these systems were controlled by software written in LabVIEW (National Instruments). Data were log-time compressed prior to fitting. Data manipulation was performed with MATLAB R2008a (Mathworks, Inc.) and graphed with Igor Pro 5.01 (Wavemetrics).

Absorption Spectra

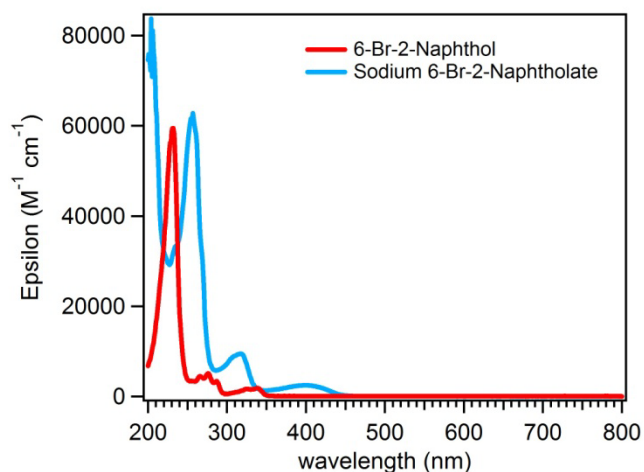


Figure S1 Absorption Spectra of 6-bromo-2-naphthol (red) and sodium 6-bromo-2-naphtholate (blue) in acetonitrile.

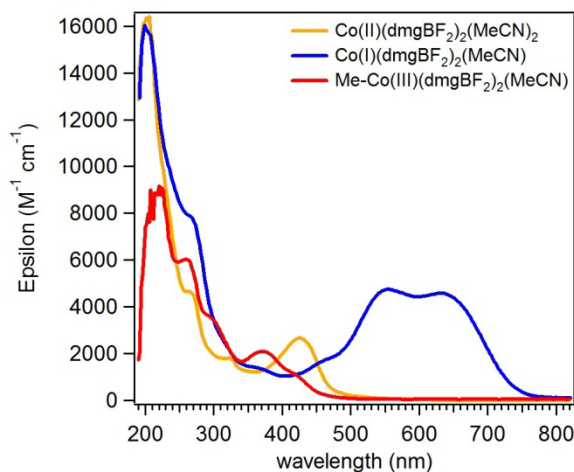


Figure S2 Absorption Spectra of Co(II)(dmgBF₂)₂(CH₃CN)₂ (yellow), [Na][Co(I)(dmgBF₂)₂(CH₃CN)] (blue), MeCo(III)(dmgBF₂)₂(CH₃CN)] (red) in acetonitrile.

Table 1 Absorption Characterization

Sample	UV-Vis Absorption/nm (Epsilon/(M ⁻¹ s ⁻¹))
6-Bromo-2-Naphthol	232 (59,450), 276 (5,111), 339 (1,851)
Sodium 6-Bromo-2-Naphtholate	257 (62,785), 316 (9,484), 402 (2,489)
Co(II)(dmgBF ₂) ₂ (CH ₃ CN) ₂	260 (4,645), 322 (1,810), 424 (2,660)
[Na][Co(I)(dmgBF ₂) ₂ (CH ₃ CN)]	264 (7,905), 553 (4,712), 628 (4,546)
Me-Co(III)(dmgBF ₂) ₂ (CH ₃ CN)	258 (6,042), 370 (2,090)

Absorption spectra at time intervals of Photolysis

A 4 mL sample in acetonitrile containing 672 μM 6-bromo-2-naphthol, 167 μM [Na][Co^I(dmgBF₂)₂(CH₃CN)], and 100 mM [NBu₄][PF₆] in a 1 cm pathlength quartz cuvette was photolyzed at 266 nm. Absorption spectra were measured at various time intervals during photolysis (Figure S3). Global analysis was performed to determine the concentrations of [Co^I(dmgBF₂)₂(CH₃CN)]⁻, Co^{II}(dmgBF₂)₂(CH₃CN)₂, and [Na][6-bromo-2-naphtholate] at each time interval (6-bromo-2-naphtholate does not absorb in the region of interest). Interestingly, the absorption of [Na][6-bromo-2-naphtholate] made up a negligible component of the spectra, while the sum of [Co²⁺] and [Co⁺] was consistently $\sim 170 \mu\text{M}$ (Table 1), suggesting a reactive pathway for the naphtholate decomposition, as observed by Pretali et al.⁵

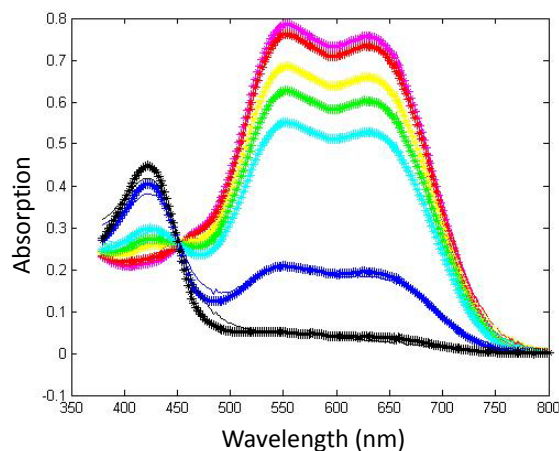


Figure S3 Absorption spectra (solid lines) and corresponding global fits (starred lines) monitored at arbitrary time points during photolysis. Sample initially contained 672 μM 6-bromo-2-naphthol, 167 μM [Na][Co(dmgBF₂)₂(CH₃CN)], and 100 mM [NBu₄][PF₆] in acetonitrile in a 1 cm pathlength cuvette. Sample 1-pink, sample 2-red; sample 3-yellow; sample 3-green; sample 4-cyan; sample 5-blue; sample 4-black.

Table 2 Sample components for each absorption measurements in Figure S3, obtained from global analysis in units of M.

Sample	[Co ^I]	[Co ^{II}]	[6-bromo-2-naphtholate]
1	1.66E-04	3.30E-06	1.88E-05
2	1.61E-04	8.80E-06	1.98E-05
3	1.45E-04	2.68E-05	1.99E-05
4	1.32E-04	3.71E-05	2.09E-05
5	1.16E-04	5.20E-05	2.22E-05
6	4.22E-05	1.19E-04	2.52E-05
7	8.30E-06	1.49E-04	2.61E-05

Luminescence Spectra of 6-Br-2-Naphthol and Sodium 6-Bromo-2-Naphtholate

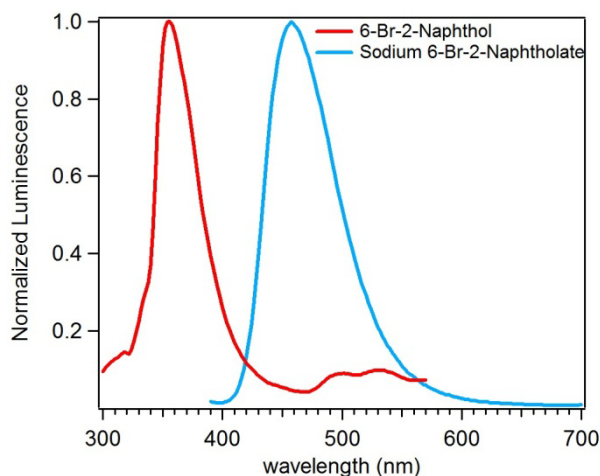


Figure S4 Normalized luminescence spectra of 6-bromo-2-naphthol (red) and sodium 6-bromo-2-naphtholate (blue), room temperature, in acetonitrile solution. λ_{ex} (6-bromo-2-naphthol) 290 nm, λ_{ex} (sodium 6-bromo-2-naphtholate) 380 nm. Weak phosphorescence at room temperature is observed for 6-bromo-2-naphthol but not sodium 6-bromo-2-naphtholate.

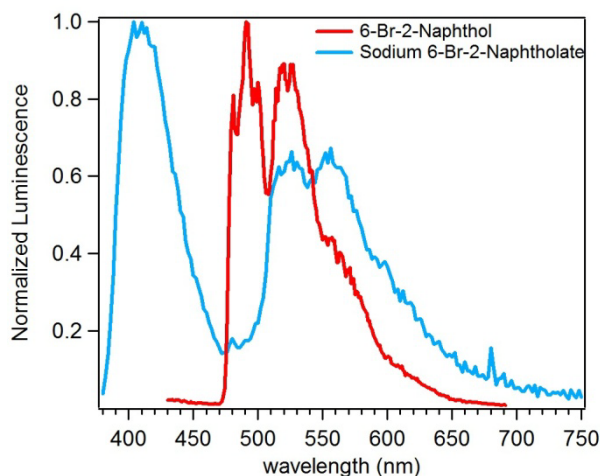


Figure S5 Normalized luminescence spectra of 6-bromo-2-naphthol (red) and sodium 6-bromo-2-naphtholate (blue), 77K, in butyronitrile glass. λ_{ex} (6-bromo-2-naphthol) 340 nm, λ_{ex} (sodium 6-bromo-2-naphtholate) 340 nm. Both fluorescence and phosphorescence were measured for sodium 6-bromo-2-naphtholate, but the fluorescence of 6-bromo-2-naphthol was not measured at 77K due to experimental limitation.

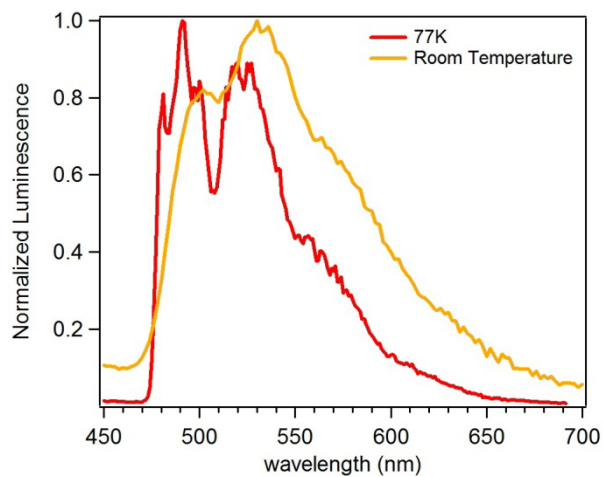


Figure S6 Normalized phosphorescence spectra of 6-bromo-2-naphthol at 77K (red, in butyronitrile glass) and at room temperature (orange, in acetonitrile solution). λ_{ex} (77K) 340 nm, λ_{ex} (room temperature) 290 nm.

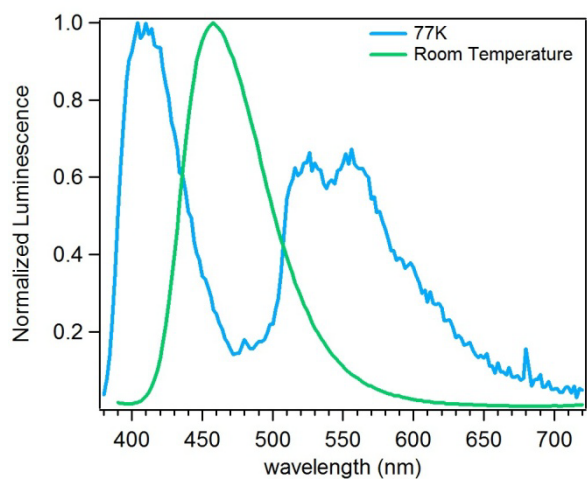


Figure S7 Normalized luminescence spectra of sodium 6-bromo-2-naphtholate at 77K (blue, in butyronitrile glass) and at room temperature (green, in acetonitrile solution). λ_{ex} (77K) 340 nm, λ_{ex} (room temperature) 380 nm.

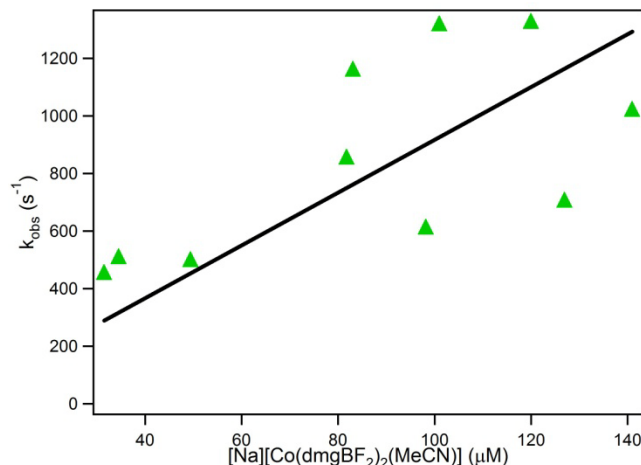


Figure S8 The slow kinetics process of kinetics traces measured at 630 nm was fit to a biexponential decay. The larger rate constant exhibits a linear relationship with the concentration of $[\text{Co}(\text{dmgbF}_2)_2(\text{CH}_3\text{CN})]^-$. All samples contained 600 μM 6-bromo-2-naphthol, 100 mM $[\text{NBu}_4][\text{PF}_6]$ and a varying concentration of $[\text{Na}][\text{Co}(\text{dmgbF}_2)_2(\text{CH}_3\text{CN})]$. A linear fit to the data series, $k_{\text{obs}} = k_{\text{red}}^*[\text{Co}(\text{dmgbF}_2)_2(\text{CH}_3\text{CN})]^-$, gives $k_{\text{red}} = 9.2 \times 10^6 \text{ M}^{-1} \text{ s}^{-1}$.

3. Calculations of Ground State and Excited State pK_a Values

pK_a of 6-Bromo-2-Naphthol in CH_3CN

The pK_a of 6-bromo-2-naphthol in DMSO has been reported as 16.2.⁶ The pK_a of 6-bromo-2-naphthol in CH_3CN can be estimated from the DMSO value by the method of Koppel and coworkers, shown in equation 1.⁷

$$pK_a \text{ of 6-bromo-2-naphthol in } \text{CH}_3\text{CN} = 11.80 + 0.884(pK_a(\text{DMSO})) = 26.1 \text{ (Eq. 1)}$$

pK_a^* of 6-Bromo-2-Naphthol in CH_3CN

The Förster cycle⁸⁻⁹ was used to estimate the pK_a^* of 6-bromo-2-naphthol, $pK_a - pK_a^* = (E_{\text{HA}} - E_{\text{A}^-})/(2.3k_{\text{B}}T)$. For *1pK_a , E_{HA} and E_{A^-} are the difference between S_0 and S_1 ($E_{0,0}$) in wavenumbers. For *1pK_a , $E_{0,0}$ is estimated from the intersection of normalized absorption and fluorescence spectra of the naphthol and naphtholate, and converted to wavenumbers. For *3pK_a , E_{HA} and E_{A^-} are the difference between S_0 and T_1 ($E_{0,0}$) in wavenumbers. $E_{0,0}$ is estimated from the highest energy of the structured emission observed in the low temperature phosphorescence spectra.

Table 3 Absorption and Fluorescence Maxima in CH_3CN at Room temperature

	Abs Max (cm^{-1})	Fluorescence Max (cm^{-1})	$E_{0,0}$ (cm^{-1})
$^{\text{Br}}\text{NaphOH}$	29,586	28,090	29,070
$[\text{Na}^+][^{\text{Br}}\text{NaphO}^-]$	24,876	21,834	23,148
$E_{\text{HA}}-E_{\text{A}^-}$	4,710	6,256	5,922

Table 4 Phosphorescence data in butyronitrile at 77K

	$E_{0,0}$ (cm^{-1})
$^{\text{Br}}\text{NaphOH}$	20,790
$[\text{Na}^+][^{\text{Br}}\text{NaphO}^-]$	19,379
$E_{\text{HA}}-E_{\text{A}^-}$	1,411

Table 5 Excited State pK_a values in CH_3CN estimated from the Förster Cycle

Excited State	$E_{\text{HA}^-} - E_{\text{A}^-}$ calculated from	Temperature (K)	pK_a^*
Singlet	Fluorescence Maxima	298	13.0
Singlet	Fluorescence $E_{0,0}$	298	13.7
Triplet	Phosphorescence $E_{0,0}$	77	14.6

Estimates of pK_a^* of 6-Bromo-2-Naphthol in CH_3CN coupled to excited state relaxation

The Förster cycle⁸⁻⁹ estimates the pK_a of *1,3 [6-bromo-2-naphthol] upon deprotonation to *1,3 [6-bromo-2-naphtholate]. However, the pK_a is expected to be significantly lower if the deprotonation is coupled with relaxation of the excited state. The predicted pK_a of the triplet state is estimated from the energy cycle pictured below (Figure S9) to be approximately -26.3.

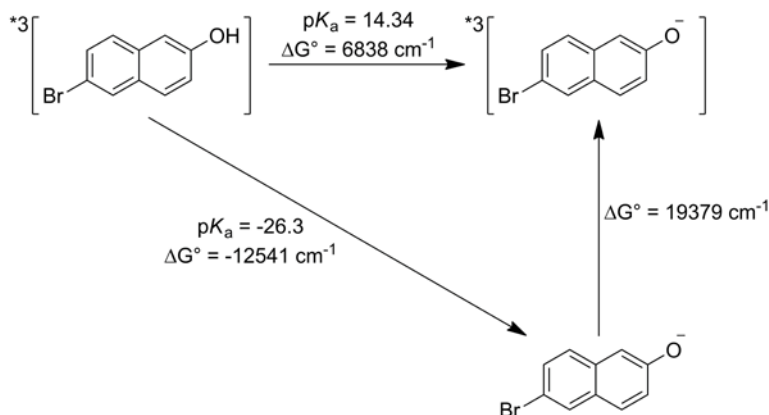


Figure S9 Energy cycle based on the Förster cycle predicted excited-state pK_a and $E_{0,0}(T_1 \leftarrow S_0)$ of 6-bromo-2-naphtholate. pK_a values were converted to free energy via $\Delta G^\circ = -k_B T \ln(K_a)$.

Quenching of 3* [6-bromo-2-Naphthol] by $[\text{NBu}_4][\text{OTs}]$

To probe the excited-state pK_a of 6-bromo-2-naphthol, quenching by the conjugate base of *p*-toluenesulfonic acid ($pK_a = 8.0$ in CH_3CN), tetrabutylammonium tosylate ($[\text{NBu}_4][\text{OTs}]$) was monitored by transient absorption measurements of 3* [6-bromo-2-Naphthol] (Figure 13). As described by Pretali et al., the decay of 3* [6-bromo-2-Naphthol] is biexponential, with rate constants of $6.4 \times 10^4 \text{ s}^{-1}$ and $4.0 \times 10^5 \text{ s}^{-1}$.⁵ In the presence of $[\text{NBu}_4][\text{OTs}]$, biexponential decays are still observed (Figure S11), with the coefficient for the larger rate constant roughly 3.3 times larger than the smaller one. Based on the larger rate constant, a second-order rate constant for proton transfer is approximately $5.1 \times 10^6 \text{ M}^{-1} \text{ s}^{-1}$.

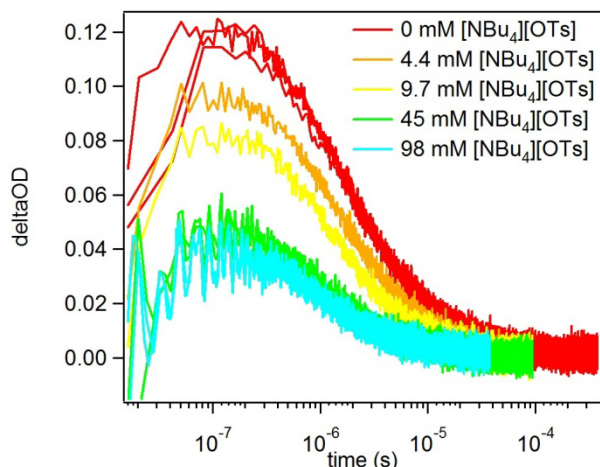


Figure S10 Kinetics traces monitoring the absorption of $^3\epsilon$ [6-bromo-2-naphthol] at 460 nm ($\lambda_{ex} = 266$ nm) with varying concentrations of $[NBu_4][OTs]$. Kinetics traces are best fit to biexponential decay kinetics.

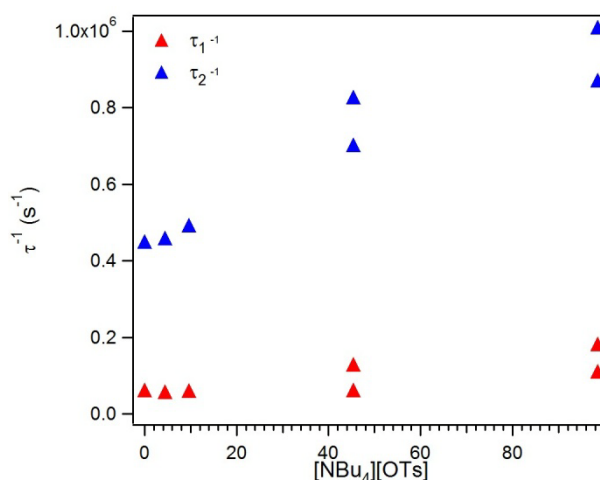


Figure S11 Rate constants for the biexponential decay of $^3\epsilon$ [6-bromo-2-naphthol] in the presence of $[NBu_4][OTs]$.

4. Hydrogen Evolution Yields from Bulk Photolysis

Experimental Details

Bulk photolysis experiments were utilized to characterize the evolution of hydrogen from excitation of 6-bromo-2-naphthol in the presence of $[Na][Co(dmgBF_2)_2(CH_3CN)]$. Reactions were run in a custom built 61 mL round bottom flask fitted with a 1 inch diameter quartz window, 24/40 ground glass joint, Kontes valve leading to a 14/20 joint sealed with a septum. In a glovebox, the reaction vessel was charged with 5 mM 6-bromo-2-naphthol, 50 mM NBu_4PF_6 , and the noted amount of $[Na][Co(dmgBF_2)_2(CH_3CN)]$ in 40 mL acetonitrile with a stirbar and the vessel was sealed with a 24/40 glass stopper and Kontes valve. The sample was placed in front of a ~100 mW 266 nm Nd:YAG laser and photolyzed while stirring for approximately 45 minutes until the blue $[Na][Co(dmgBF_2)_2(CH_3CN)]$ had reacted to form yellow $Co(dmgBF_2)_2(CH_3CN)_2$.

The amount of H_2 produced evolved was quantified by analyzing the gas mixture in the headspace using an Agilent 7890A GC-TCD. The total amount of H_2 produced was calculated as

a sum of the H₂ in the headspace plus the H₂ dissolved in the solvent (calculated using Henry's Law with a constant of 290 L•atm/mol).

Table 6 Hydrogen evolution yields from bulk photolysis experiments

Run	[Co(dmgBF ₂) ₂ (CH ₃ CN)] (μM)	% H ₂ in Headspace	% Yield
1	510	0.65	64
2	446	0.39	38

5. Calculations of Barriers

Barriers were estimated as:

$$\Delta G^\ddagger = -RT \ln \left(\frac{k}{Z} \right)$$

k = rate constant, M⁻¹ s⁻¹

Z = collision factor, 10¹¹ M⁻¹ s⁻¹

R = molar gas constant, 0.001986 kcal K⁻¹ mol⁻¹

T = temperature, 298 K

References Cited

- (1) Pangborn, A. B.; Giardello, M. A.; Grubbs, R. H.; Rosen, R. K.; Timmers, F. J. *Organometallics* **1996**, *15*, 1518.
- (2) Bakac, A.; Espenson, J. H. *J. Am. Chem. Soc.* **1984**, *106*, 5197.
- (3) Ram, M. S.; Riordan, C. G.; Yap, G. P. A.; LiableSands, L.; Rheingold, A. L.; Marchaj, A.; Norton, J. R. *J. Am. Chem. Soc.* **1997**, *119*, 1648.
- (4) Hu, X.; Brunschwig, B. S.; Peters, J. C. *J. Am. Chem. Soc.* **2007**, *129*, 8988.
- (5) Pretali, L.; Doria, F.; Verga, D.; Profumo, A.; Freccero, M. *J. Org. Chem.* **2009**, *74*, 1034.
- (6) Bordwell, F. G.; Cheng, J. *J. Am. Chem. Soc.* **1991**, *113*, 1736.
- (7) Kütt, A.; Leito, I.; Kaljurand, I.; Sooväli, L.; Vlasov, V. M.; Yagupolskii, L. M.; Koppel, I. A. *J. Org. Chem.* **2006**, *71*, 2829.
- (8) Grabowski, Z. R.; Rubaszewska, W. *J. Chem. Soc., Faraday Trans. 2* **1977**, *73*, 11.
- (9) Forster, T. Z. *Elektrochem.* **1950**, *54*, 531.